Report

Cell Reports

The Edges of Pancreatic Islet β Cells Constitute Adhesive and Signaling Microdomains

Graphical Abstract

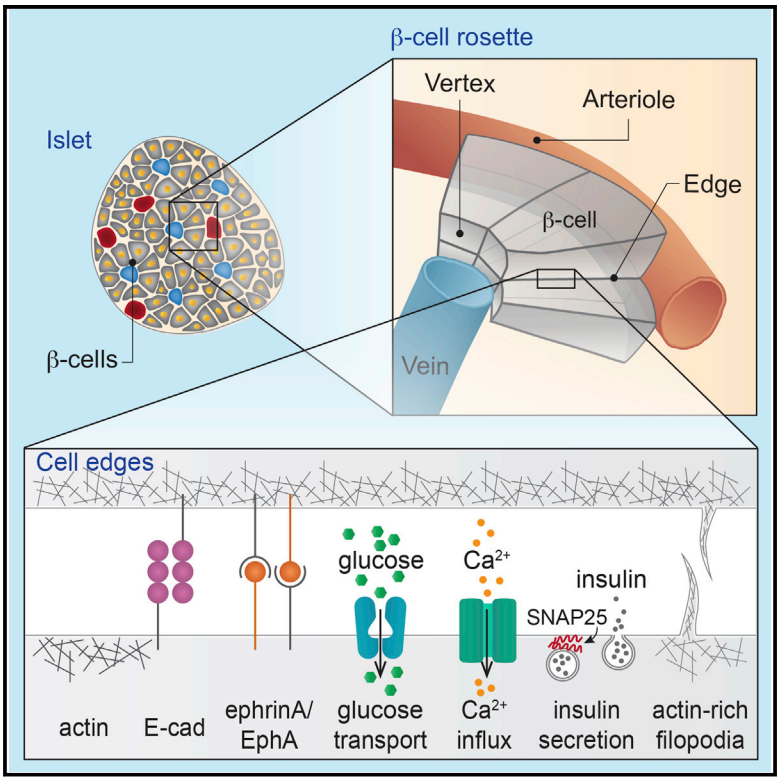

Highlights

- Pancreatic β cells meet at sharp angles to form distinct edges
- Murine β cell edges display high levels of F-actin and E-cadherin
- Edges are also enriched in signaling molecules, generating polarized microdomains
- Human β cells show similar edge organization, underscoring functional significance

Authors

Erez Geron, Sigalit Boura-Halfon, Eyal D. Schejter, Ben-Zion Shilo

Correspondence

benny.shilo@weizmann.ac.il

In Brief

Pancreatic islet β cells secrete insulin in response to glucose uptake. Whereas β-cell organization within islets is well characterized, it is not known how each cell is polarized. Geron et al. demonstrate that contact points between β cell edges represent functional domains, where the machinery for importing glucose and secreting insulin is concentrated.

Geron et al., 2015, Cell Reports *10*, 317–325
January 20, 2015
http://dx.doi.org/10.1016/j.celrep.2014.12.031

Cell Reports
Report

The Edges of Pancreatic Islet β Cells Constitute Adhesive and Signaling Microdomains

Erez Geron,[1] Sigalit Boura-Halfon,[2] Eyal D. Schejter,[1] and Ben-Zion Shilo[1,*]
[1]Department of Molecular Genetics
[2]Department of Molecular Cell Biology
Weizmann Institute of Science, Rehovot 76100, Israel
*Correspondence: benny.shilo@weizmann.ac.il
http://dx.doi.org/10.1016/j.celrep.2014.12.031

SUMMARY

Pancreatic islet β cells are organized in rosette-like structures around blood vessels and exhibit an artery-to-vein orientation, but they do not display the typical epithelial polarity. It is unclear whether these cells present a functional asymmetry related to their spatial organization. Here, we identify murine β cell edges, the sites at which adjacent cell faces meet at a sharp angle, as surface microdomains of cell-cell adhesion and signaling. The edges are marked by enrichment of F-actin and E-cadherin and are aligned between neighboring cells. The edge organization is E-cadherin contact dependent and correlates with insulin secretion capacity. Edges display elevated levels of glucose transporters and SNAP25 and extend numerous F-actin-rich filopodia. A similar β cell edge organization was observed in human islets. When stimulated, β cell edges exhibit high calcium levels. In view of the functional importance of intra-islet communication, the spatial architecture of their edges may prove fundamental for coordinating physiological insulin secretion.

INTRODUCTION

β cells of the pancreatic islets of Langerhans play a cardinal role in mediating glucose homeostasis. These cells sense minute changes in glucose blood concentrations and uptake it via the glucose transporter GLUT2 (Ashcroft and Rorsman, 2012; Thorens et al., 1988). Within β cells, glucose metabolism is coupled to depolarization of the plasma membrane that triggers insulin release (Ashcroft and Rorsman, 2012; Henquin, 2009). Adhesion between clusters of β cells regulates both basal and glucose-stimulated insulin secretion (Halban et al., 1982; Hauge-Evans et al., 1999; Konstantinova et al., 2007; Meda et al., 1990). The intricate coordination between the adhesive, sensory, and secretory capacities of β cells raises the question of how these functions are compartmentalized within the cell.

Although β cells are derived from epithelial tissue, they do not display the typical epithelial apical-basal cell polarity. In contrast to polarized tubular epithelia constituting secretory glands, β cells are exposed to a relatively homogenous extracellular environment and do not form a lumen or display obvious membranal segregation (Kasai et al., 2010; Konstantinova and Lammert, 2004). In rodents, β cells are shaped as truncated pyramids that are clustered in rosette-like structures around blood vessels (illustrated in Figure 1A; Bonner-Weir, 1988; Weir and Bonner-Weir, 1990). The artery-to-vein axis constitutes the basis for β cell orientation: the rosette is encircled by an arteriole at its periphery and is drained by a vein located at its center. The β cell nucleus is positioned close to its base, at the vicinity of the artery; the primary cilia extends laterally (Granot et al., 2009); and insulin granules are enriched at the vertex, next to the vein (Bonner-Weir, 1988). Enhanced insulin secretion at the membrane facing the vein was recently demonstrated (Low et al., 2014).

In the absence of global external polarity cues, could β cell compartmentalization be directed by local interactions with neighboring cells? By labeling individual β cells embedded within murine and human isolated islets, we were able to visualize the β cell topology, localize molecular elements within them, and record their behavior following various treatments. We identify the edges of β cells, sites where pairs of adjacent faces meet at a sharp angle, as distinct surface microdomains. The edges are aligned between neighboring cells and are positioned near large reservoirs of the extracellular fluid. Localization of adhesion, sensing, and secretion elements to the β cell edges indicates that this compartment serves as a hub for cell-cell contact and signaling.

RESULTS

The Edges of Pancreatic β Cells as F-Actin-Rich Domains

The distribution of microfilament-based structures serves as a fundamental feature and indicator of cytoplasmic and membrane domain organization and function. In order to identify actin structures within β cells at high resolution, we introduced the F-actin probe Lifeact-GFP into isolated islets, by adeno (Ad)-viral infection (Geron et al., 2013; Riedl et al., 2008). Infection was carried out shortly after islet isolation, and imaging commenced after 24 hr (see Supplemental Experimental Procedures). Islets chosen for experiments displayed a relatively smooth and rounded surface and were devoid of a necrotic center. Isolated

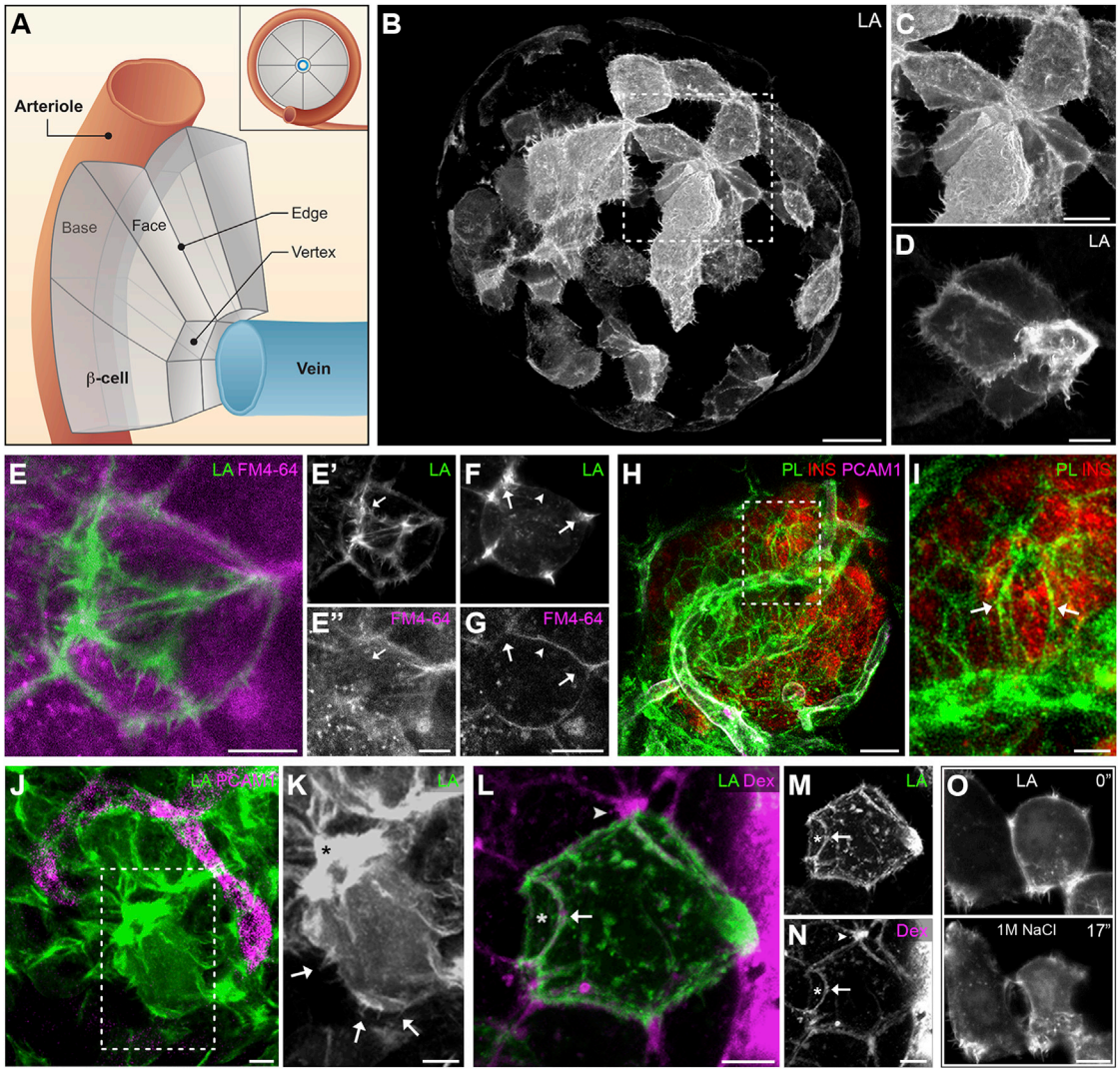

Figure 1. Lifeact-GFP Labeling Identifies the Edges of Pancreatic β Cells as F-Actin-Rich Domains and Marks Emanating Filopodia

(A) Schematic illustration of a pancreatic islet rosette. The β cells that compose each rosette are shaped as truncated pyramids, whose bases face an arteriole that circles the rosette periphery, whereas their vertices face a vein at the rosette center. Inset shows a cross section of an entire rosette.

(B and C) Live pancreatic islet (B) and rosette (C) expressing Lifeact-GFP (LA) (gray). (C) is an enlargement of the boxed region in (B). Note that the sharp cell edges are aligned between neighboring cells. Pancreatic islets shown in this and subsequent panels and figures were infected with Ad-Lifeact-GFP for 2 hr, washed, and cultured for 24 hr before initiation of imaging. Use of other protocols is specifically stated.

(D) Representative β cell expressing Lifeact-GFP (gray) displays enhanced F-actin and numerous emanating filopodia at its edges and vertex.

(E–G) Live β cell expressing Lifeact-GFP (green, gray), stained with the lipophilic dye FM4-64 (magenta, gray). (E)–(E'') are maximal intensity projections of consecutive optical sections, whereas (F) and (G) are separated channels of a single section. Note that the Lifeact-GFP signal (E' and F) is much more pronounced at the edges (arrows) than along the cell faces (arrowhead), whereas the membrane marker (E'' and G) displays a uniform distribution.

(H and I) Whole-pancreas fragment from a C57B6 mouse stained for F-actin (phalloidin [PL]; green), insulin (INS) (red), and PCAM1 (magenta). Pancreata were excised without enzymatic digestion, minced, and immediately fixed. Pancreatic fragments were then stained with the indicated antibodies. (I) is an enlargement of the boxed region in (H). Arrows in (I) point to β cell edges.

(J and K) Whole-pancreas fragment from a Lifeact-GFP-transgenic mouse (green; gray) stained for PCAM1 (magenta). Sample was produced as in (H). Note the blood vessel that circles the rosette periphery in (J). (K) is an enlargement of the boxed region in (J). Arrows in (K) point to β cell filopodia. Asterisk marks enhanced F-actin localization at the vertex.

(L–N) β cells expressing Lifeact-GFP (green; gray), immersed in medium supplemented with fluorescent dextran (Dex) (magenta; gray). Pancreatic islets were infected, washed, and resuspended in the presence of extracellular dextran before the initiation of imaging. The high-intensity dextran signal at the right sides of images (L) and (N) is the dextran-supplemented medium surrounding the islet. Arrows point to a reservoir of medium-borne dextran at a junction of edges from neighboring cells. Asterisks mark a dextran-free cellular face, and arrowheads point to pronounced dextran enrichment at junctions of three or more edges from neighboring cells.

(O) Time series of β cells expressing Lifeact-GFP (gray), exposed to 1 M NaCl at t = 0 s. Note that, upon treatment, β cells pulled away from their neighbors at their faces but remained attached to them at their edges.

Cells in (D), (J), and (K) were insulin positive (not shown). The scale bars represent 20 μm (B and H), 10 μm (C), and 5 μm (D, E, G, I–L, N, and O).

islets retained their ability to secrete insulin in response to various stimuli, such as glucose and KCl, even after viral infection (Figures S1C and S2D; Carter et al., 2009).

Lifeact-GFP infection resulted in labeling of a small percentage of the islet cells, mainly within the outer four layers (Figure 1B; Movie S1). More than 90% of these Lifeact-GFP-expressing cells were β cells, as demonstrated by staining for different islet cell markers (Figures S1A and S1B). Notably, the ability to infect only some of the cells within an islet provided a sharp contrast for visualizing the morphology and boundaries of pancreatic β cells.

Imaging of islets infected with Ad-Lifeact-GFP allowed clear visualization of pancreatic β cells. The cells appeared as elaborated truncated pyramids with 7–15 faces (Figures 1B–1D). Labeling of several β cells also allowed visualization of the rosettes they compose, where the β cell bases are oriented toward the rosette periphery and their narrow top, or vertex, toward the rosette center (Figures 1A–1C; Bonner-Weir, 1988). Identification of pancreatic rosettes was also aided by localization of endothelial markers such as laminin and PCAM1 (Figure S3A). Importantly, F-actin enrichment was prominent at cortical sites where adjacent cell faces meet at a sharp angle, herein referred to as cell edges (Figures 1B–1D). At the cell vertex facing the vein, where a number of edges meet, F-actin is particularly enriched (Figure 1D). In addition, F-actin also marked fine filopodial structures that emanate exclusively from the cell edges and vertices (Figure 1D).

The observed enrichment of microfilaments is not a consequence of excess membrane at the edges, because simultaneous labeling of the plasma membrane with the lipophilic dye FM4-64 resulted in roughly uniform staining of all membrane aspects, including the cell edges (Figures 1E–1G). To verify these observations in a quantitative manner, we compared the fluorescent intensities of the F-actin and membrane probes at the β cells edges versus their adjacent faces and generated an edge-to-face enrichment index. Indeed, the Lifeact-GFP intensity was 6-fold higher at the edges, whereas the FM4-64 dye was not significantly enriched at these areas (see Experimental Procedures for criteria used). The β cell edge organization was also apparent at borders with neighboring non-β cells (Figures S3B and S3C).

We next tested whether the enrichment of F-actin at the β cell edges of isolated islets represents their native actin organization. To this end, whole-pancreas fragments were produced without enzymatic digestion and were fixed shortly after excision, resulting in intact organization of the islets, including the surrounding tissue and the connecting blood vessels (Figures 1H and 1J). F-actin enrichment at β cell edges was readily observed when such preparations were stained with the conventional F-actin probe phalloidin (Figures 1H and 1I) and in similar pancreatic preparations from Lifeact-GFP-transgenic mice, which also allowed for the detection of β cell filopodia (Figures 1J and 1K, arrows). In addition, this type of preparation facilitated visualization of pancreatic rosettes in relation to the blood capillaries that surround them and the enhanced F-actin localization at β cell vertices, which orient toward the center of the rosette (Figures 1J and 1K).

Cell-Cell Contact at the Edges

β cells display an edge-to-edge alignment with adjacent cells (Figures 1B and 1C). This contact region between neighboring β cells was hypothesized to serve as a canalicular system, in which the interstitial fluid flows along the artery-to-vein axis (Weir and Bonner-Weir, 1990). To test if the extracellular fluid is indeed more accessible to the cells at their edges, we immersed isolated islets in medium supplemented with a 10 kD fluorescent dextran (Takahashi et al., 2002). Notably, the interstitial spaces adjacent to the cell edges appeared as greater reservoirs of medium-borne dextran than those adjacent to the cell faces (Figures 1L and 1M, arrows and asterisks, respectively). This enrichment was pronounced at junctions of three or more edges from neighboring cells (Figures 1L and 1N, arrowheads).

The consistent alignment observed between edges of neighboring β cells suggested that they provide an adhesive domain between cells. To test this notion, we shrunk the cells by exposing islets to a hypertonic NaCl solution. Upon such treatment, shrinking β cells, visualized by Lifeact-GFP, pulled away from their neighbors at their faces but remained attached to them at their edges (Figure 1O).

We next tried to disrupt the β cell edge organization. We found that chelating calcium (Ca^{2+}) by EDTA led to a gradual reduction of F-actin at the β cell edges and to its redistribution throughout the cell cortex (Figure 2A; Movie S2). Concomitantly, labeled β cells lost their polyhedron shape, became round, and pulled away from their neighbors, leading to inflation in the islet volume (Figures 2A and S4; Movie S2). When the Ca^{2+} chelator was removed, the edge organization of β cells was restored within ~90 min. Recovered β cells re-established their typical shape and returned to display faces, edges, and vertices (Figure 2B; Movie S3). In parallel, fully recovered islets regained their ability to secrete insulin in response to a glycemic stimulus, which was impaired during the early stages of recovery (Figure 2C). These observations imply a role for β cell edges and contact in insulin secretion.

E-cadherin (Ecad), a cell-surface protein commonly associated with Ca^{2+}-dependent adhesive functions, was shown to mediate adhesion between β cells and influence their insulin secretory capacity (Carvell et al., 2007; Dahl et al., 1996). Immunofluorescence staining revealed that Ecad localizes preferentially at β cell edges and filopodia (Figures 2D and 2E), suggesting that the edge-to-edge adhesiveness we observed may be mediated by Ecad. To test the role of Ecad in edge re-establishment, we allowed EDTA-treated islets to recover in the presence of either anti-Ecad or isotype control antibodies. β cells in the control group compacted and regenerated a typical polyhedron shape with faces, edges, and vertices, as monitored by Lifeact-GFP (Figures 2F and S4; Movie S4). However, β cells treated with anti-Ecad antibodies remained static, did not compact, and failed to display comparable face and edge re-establishment (Figures 2G and S4; Movie S4). These observations imply that reformation of β cell edges following EDTA disruption depends on establishment of new Ecad-Ecad interactions.

Notably, the inability to restore edge organization following anti-Ecad antibody treatment was associated with impaired glucose-stimulated insulin secretion (Figure 2H). Treating islets with anti-Ecad antibodies without pre-exposure to EDTA did not alter their edge organization or their insulin secretion capacity (Figures 2H and 2I). In conclusion, loss of Ca^{2+}/Ecad-dependent edge organization is clearly associated with a reduction in insulin secretion, implying a functional role for the β cell edges.

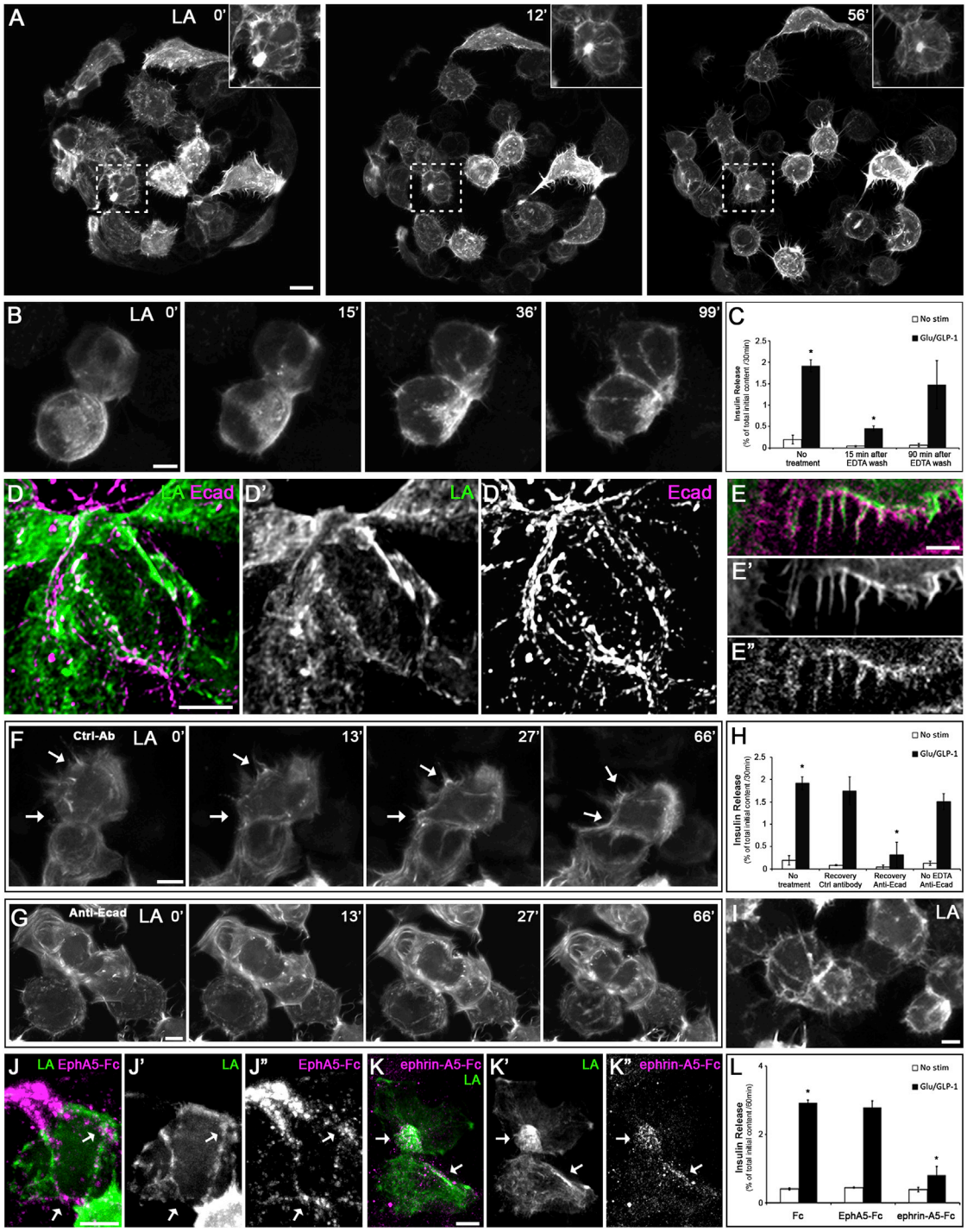

Figure 2. Pancreatic β Cell Edge Organization Is Contact and E-Cadherin Dependent and Correlates with Insulin Secretion

(A) Time series of islet expressing Lifeact-GFP (LA, gray) before and during exposure to 5 mM EDTA. Islets were infected, washed, and exposed to EDTA at t = 0. Note the loss of β cell edges, redistribution of F-actin throughout the cell cortex, and the dissociation of neighboring cells accompanied by islet volume inflation. Inset is a 2× magnification of the boxed area.

(B) Time series of β cell expressing Lifeact-GFP (gray) following EDTA wash. Islets were infected, exposed to 5 mM EDTA for 40 min, washed thoroughly, and imaged during recovery. Note the re-establishment of edges and polyhedron shape.

(C) Insulin release from nontreated and EDTA-treated islets. Treated islets were exposed to 5 mM EDTA for 40 min, washed thoroughly, and incubated for 30 min in 3 mM glucose (No stim) or 20 mM glucose supplemented with 10 nM GLP-1(Glu/GLP-1), either 15 or 90 min after EDTA wash. Results represent the average and SEM of two to four independent experiments (sets of mice). $p = 5 \times 10^{-3}$, unequal variance, t test (two tailed).

(legend continued on next page)

Contact between β cells facilitates direct binding and signaling of the EphA5 receptor tyrosine kinase with its ephrin-A5 ligand, leading to regulated insulin secretion (Konstantinova et al., 2007). Use of EphA5-Fc and ephrin-A5-Fc fusion proteins, which bind to their cognate partners, allowed mapping the localization of the endogenous components with respect to the edges. Importantly, both the ephrin-A ligands and EphA receptors localized to punctuate structures, which are enriched at the β cell edges and vertices (Figures 2J and 2K, arrows), and ephrin-A5-Fc reduced glucose-stimulated insulin secretion from islets, whereas EphA5-Fc did not show an effect on intact islets (Figure 2L). These results highlight the edges as main contact sites between adjacent β cells.

Signaling and Secretion Elements Are Enriched at the Edges

We next asked whether the β cell edges are enriched in key elements required for environmental sensing and insulin secretion. Notably, the glucose transporter GLUT2 (Orci et al., 1989) was found to be enriched at the β cell edges and vertices (Figures 3A and 3F). SNAP-25, which is a t-SNARE-mediating fusion of insulin vesicles (Sadoul et al., 1995), was found to be similarly enriched at the edges of β cells (Figures 3C and 3F). The $K_v2.1$ subunit of the voltage-dependent K^+ channel, which is responsible for repolarizing of the plasma membrane, is enhanced at the edges as well (Figures S5A and 3F). Finally, enrichment of the $Ca_v1.3$ subunit of the L-type voltage-dependent Ca^{2+} channels (Ca_V) at the cell vertices was also detected (Figures 3D–3F). In contrast, and in agreement with previous studies, $K_{ir}6.2$, the pore-forming unit of the ATP-sensitive K^+ channel, was evenly dispersed over the β cell surface (Figures S5B and 3F; Xia et al., 2004). In general, once the localization of these proteins was identified in Lifeact-GFP-expressing β cells, their typical distribution could be readily recognized in adjacent noninfected cells (Figure 3).

Besides accentuating the cell edges, visualization of β cells by Lifeact-GFP also identified numerous filopodia that extend from the edges. These extensions reach an average length of 3.3 ± 0.6 μm, whereas their width is below the diffraction limit of standard light microscopy (~200 nm). The position and dimensions of the filopodia suggest that they could correspond to the linear extensions referred to as microvilli, reported in several ultrastructure studies of pancreatic islets (Bendayan, 1992; Orci et al., 1989). Whereas the filopodial localization pattern of several membranal markers, including Ecad and GLUT2, was similar to that of the edges from which they emanate and higher than that of the β cell faces (Figures 2E and 3B), cytosolic structures such as insulin granules, ER, and mitochondria, which are present underneath the edges, are absent from the filopodia (Figures S5C–S5G). Similarly, filopodia do not contain acetylated or nonacetylated microtubules (Figures S5H–S5J). Soluble cytosolic proteins, however, were detected throughout the interior volume of the filopodia (Figure S5K). We thus consider these thin extensions as structures that contain mostly F-actin and cytoplasm.

The novel features of mouse β cells we have identified were also examined in pancreatic islets obtained from healthy human donors. β cells in human islets appeared as elaborated polyhedrons, with F-actin enriched at the cell edges, and the edges aligned between neighboring cells (Figure 4A). Similarly, Ecad and SNAP25 were found to be concentrated mostly at the β cell edges (Figures 4B-4D). Finally, prominent actin-rich filopodia emanating from the cell edges were also detected (Figures 4A and 4C, arrows). These observations suggest that the edge organization is a conserved architectural β cell module.

Elevated Ca^{2+} Influx at the Edges

Insulin secretion requires the induction of electrical activity at the β cell plasma membrane. This activity appears as action potential bursts and hyperpolarized interbursts. In mouse β cells, the action potentials are evoked mainly by Ca^{2+} influx from the extracellular space through Ca_V (Drews et al., 2010). We thus wanted to test if the edges function as microdomains for Ca^{2+} sensing and correspond to such functional domains, as was previously postulated (Rutter et al., 2006). To allow dynamic visualization of Ca^{2+} in individual β cells within intact islets, pancreatic islets were coinfected with Ad-Lifeact-GFP and Adeno-associated viruses (AAV) harboring the red-fluorescent-protein-based Ca^{2+} sensor, RCaMP1h (Akerboom et al., 2013). Coexpression of Ca^{2+}-sensitive and F-actin probes within individual β cells allowed for a ratiometric quantification of the elevation in the Ca^{2+} signal following stimulation. Islets were treated with KCl to reach extracellular concentrations of ~40 mM. Application of KCl leads to depolarization of the plasma membrane, opening of Ca_V channels, and a subsequent rise in cytosolic

(D–E") β cells expressing Lifeact-GFP (green; gray), stained for E-cadherin (Ecad) (magenta; gray). (E)–(E") display enrichment of Ecad over β cell filopodia.
(F and G) Time series of β cells expressing Lifeact-GFP (gray) following EDTA wash and during exposure to either isotype control or anti-Ecad antibodies (5 μg/ml). Islets were treated as in (B) but were exposed to the indicated antibodies during the last 10 min of EDTA treatment and during recovery. Note that the control group cells re-establish a polyhedron shape and edges (arrows), whereas the anti-Ecad-treated cells fail to do so.
(H) Insulin release after EDTA and anti-Ecad treatment. Islets exposed only to anti-Ecad antibodies were treated for an equivalent time. Results represent the average and SEM of two to four independent experiments (sets of mice). $p = 2 \times 10^{-4}$, unequal variance, t test (two tailed).
(I) Live β cells expressing Lifeact-GFP (gray) treated with anti-Ecad antibodies without prior exposure to EDTA. Islets were infected, washed, and incubated with anti-Ecad antibodies for 90 min before imaging.
(J and K) Localization of ephrin-A (J) and EphA (K) as revealed by staining with fusion proteins derived from their cognate binding partners (EphA5-Fc and ephrin-A5-Fc respectively; magenta). β cells expressing Lifeact-GFP (green; gray) were infected, and 24 hr later, the islets were washed, exposed to the indicated fusion proteins (8 μg/ml) for 40 min at 37°C, fixed, and stained. The EphA5Fc signal in (J) is stronger in the noninfected cell because this cell is closer to the surface of the islet and thus more accessible.
(L) The biological activity of ephrin-A5-Fc was verified by showing marked inhibition of glucose-stimulated insulin secretion (Konstantinova et al., 2007). Insulin release from islets treated with Fc (as control), EphA5-Fc, or ephrin-A5-Fc. Islets were pre-exposed to the indicated fusion proteins (8 μg/ml) for 40 min in the absence of a glycemic stimulus and then incubated for 60 min in 3 mM glucose (No stim) or 20 mM glucose supplemented with 10 nM GLP-1 (Glu/GLP-1) and in the presence of the indicated fusion proteins. Results represent the average and SEM of two independent experiments (sets of mice). $p = 1 \times 10^{-3}$, unequal variance, t test (two tailed).
Cells in (D), (E), (J), and (K) were insulin positive (not shown). The scale bars represent 10 μm (A), 5 μm (B, D, F, G, and I–K), and 2 μm (E).

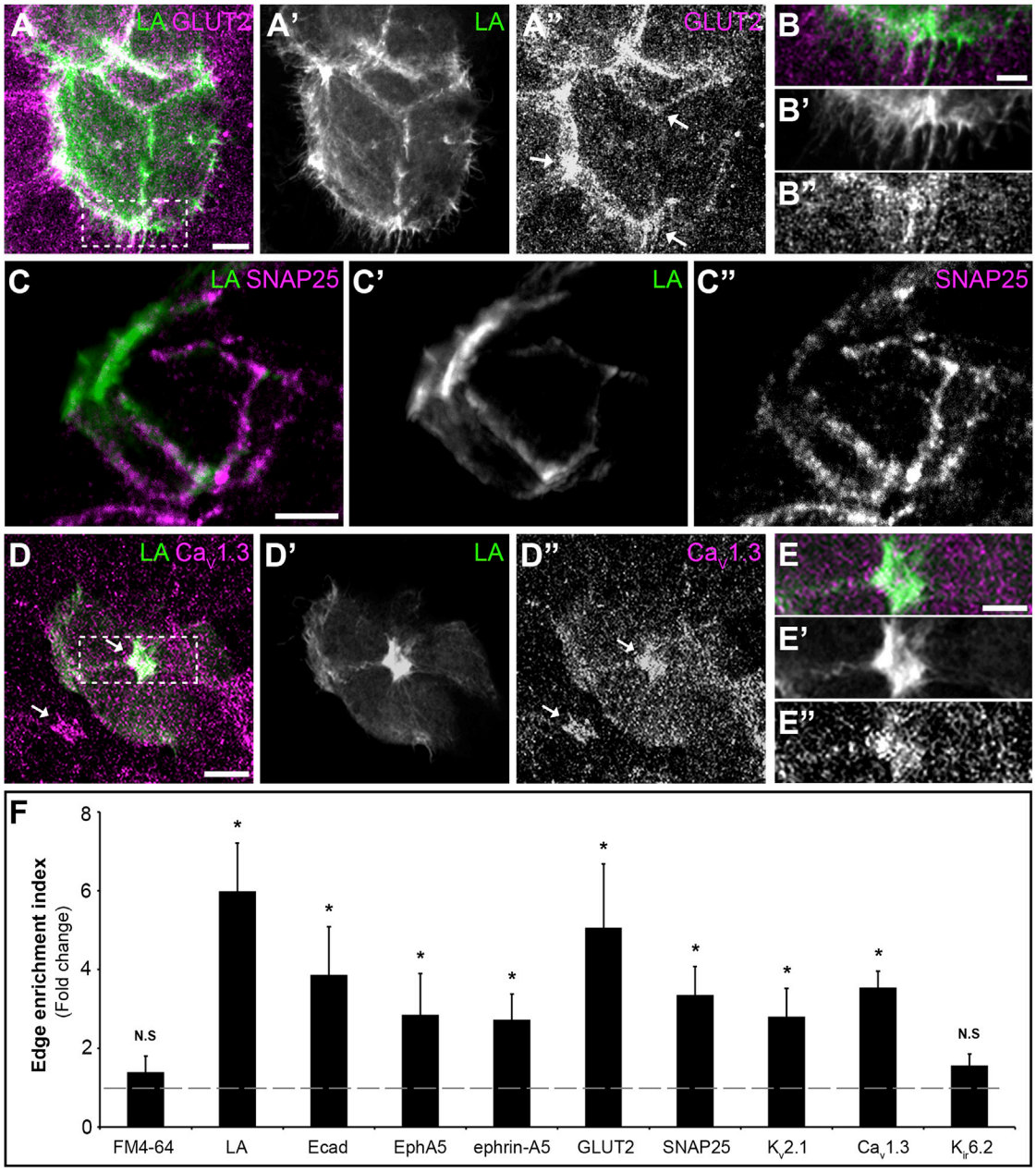

Figure 3. Pancreatic β Cell Edges Are Enriched in Sensing and Secretory Elements

(A–B") β cells expressing Lifeact-GFP (LA; green, gray), stained for the glucose transporter GLUT2 (magenta; gray). Note the enhanced concentration of GLUT2 at the edges (arrows). (B)–(B") are enlargements of the boxed region in (A).

(C–C") β cells expressing Lifeact-GFP (green; gray), stained for SNAP25 (magenta; gray).

(D–E") β cells expressing Lifeact-GFP (green; gray), stained for the Ca^{2+} channel subunit $Ca_v1.3$ (magenta; gray). Note the enhanced concentrations of $Ca_v1.3$ (arrows in D) at the vertices in both Lifeact-GFP-labeled and nonlabeled β cells. (E)–(E") are enlargements of the boxed region in (D).

(F) Ratio of fluorescent signal between β cell edges and areas between edges. Results represent the average fold change and SD; $p < 1 \times 10^{-4}$, t test (two tailed); N.S, nonsignificant; n = 30–40 edges and nonedges from at least ten β cells imaged in three to five independent experiments. Ratio of EpA and ephrin-A was determined by the binding of ephrin-A5-Fc and EphA5-Fc, respectively.

Cells in (C) and (D) were insulin positive (not shown). The scale bars represent 5 μm (A, C, and D) and 2 μm (B and E).

Ca^{2+} concentrations and insulin secretion (Gembal et al., 1992; Henquin, 2009; Ohara-Imaizumi et al., 2009). Thus, KCl administration mimics several key steps in the activation of β cells by glucose (Henquin, 2009).

Following KCl application, pancreatic cells coexpressing Lifeact-GFP and RCaMP1h displayed a global cytoplasmic and nuclear increase of approximately 70% in Ca^{2+} levels, as measured by changes in RCaMP1h intensity (Figure 5A; Ma

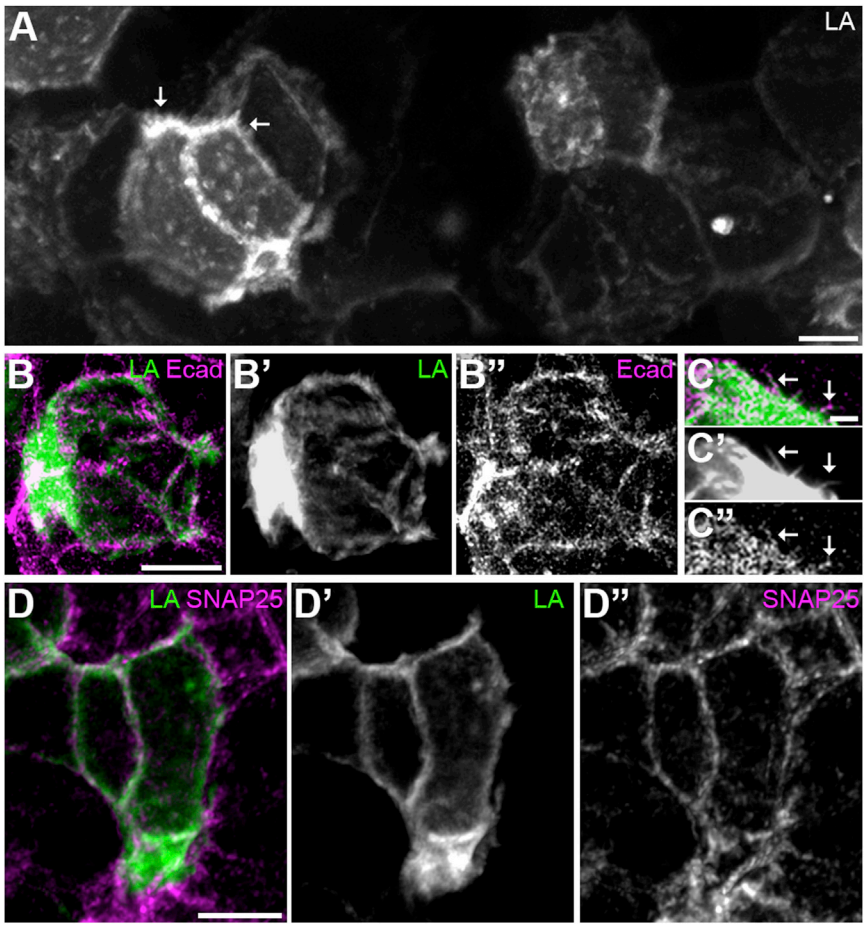

Figure 4. Human β Cell Edge Organization

(A) Live human pancreatic islet expressing Lifeact-GFP (LA, gray). Islets were infected for 2 hr, washed, and cultured for 48 hr before imaging. Note the enrichment of F-actin at the edges, the filopodia that emanate from them (arrows), and the alignment of edges between neighboring cells.

(B–C") Human β cells expressing Lifeact-GFP (green; gray), stained for Ecad (magenta; gray). (C)–(C") display enrichment of Ecad over β cell filopodia (arrows).

(D–D") Human β cells expressing Lifeact-GFP (green; gray), stained for SNAP25 (magenta; gray). Cells in (B), (C), and (D) were insulin positive (not shown). The scale bars represent 10 μm (A), 5 μm (B and D), and 2 μm (C).

et al., 2014). The elevation of Ca^{2+} levels was not uniform, however, and appeared to be pronounced at the cell edges (Figure 5A; Movie S5). This bias can be readily observed when the changes in RCaMP1h intensities at the edges and adjacent nonedge cortical segments are plotted as kymographs (Figure 5B). To quantify the changes in RCaMP1h intensities over the entire β cell cortex, we imaged islets before and after KCl application through most of the islet volume. This analysis demonstrated that the increase in Ca^{2+} indicator levels was indeed consistently greater below the edges and vertices when compared with regions below adjacent flat areas of the membrane (Figures 5C and 5D). The edges and vertices displayed an increase ($\Delta f/f_0$) that was 2-fold greater on average than adjacent flat cortical areas (Figures 5C–5F; see Supplemental Experimental Procedures for criteria used). The elevated response to Ca^{2+} at the edges highlights the functional significance of these microdomains.

DISCUSSION

Polarized secretory epithelial cells segregate their sensory and secretory functions to their basolateral and apical domains, respectively. Such strict segregation of function suits the need of polarized epithelia to act on two distinct environments: the body interior and the external world. In contrast, pancreatic β cells are only exposed to the body's interior and do not exhibit strict polarization. Pancreatic β cells utilize a different approach for subcellular organization and appear to localize their sensory and secretory functions to similar locations—their edges and vertices. Although the edges of pancreatic β cells constitute only a small portion of their perimeter, we suggest that they play a central physiological role. This is achieved by localizing adhesion, sensory, and secretory elements to the same domain, which is also exposed to larger volumes of the extracellular fluid. The prominent accumulation of F-actin at these regions raises the question of the roles that the cytoskeleton may play in assembling or maintaining edge features.

The concentration of Ecad and ephrin/Eph at the cell edges highlights their importance as hubs of cell-cell contact. What may be the advantage of colocalizing the sensory and secretory functions within the same microdomain? Because uptake of glucose and its subsequent metabolism are biochemically linked to insulin secretion, coupling these processes spatially may lead to efficient translation of glucose uptake to insulin secretion. This will increase β cell sensitivity to external cues and the ability to match the secretory response to the stimulatory magnitude. In addition, this spatial coupling may minimize the reaction time for the initiation and termination of secretion.

Although it is clear that β organization is correlated with the artery-to-vein axis (Bonner-Weir, 1988), little is known on how β cells are assembled into rosettes and how these structures are maintained. In agreement with previous studies (Carvell et al., 2007; Dahl et al., 1996), our work demonstrates the importance of homotypic Ecad interactions for β cell morphology and whole-islet architecture. Concentrating adhesiveness to the edges facilitates edge-to-edge alignment and may provide a nucleation site for membrane microdomains. In addition, alignment of neighboring edges leads to close apposition of β cell active domains. Connections between β cells by gap junctions

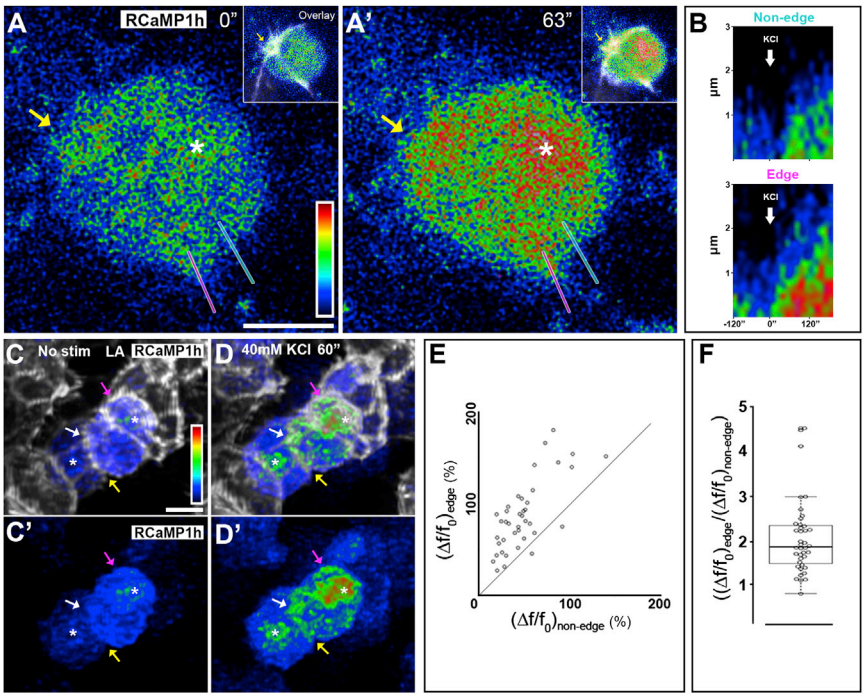

Figure 5. Pancreatic β Cell Edges Constitute Ca^{2+}-Sensing Microdomains

(A and B) β cell expressing the Ca^{2+} indicator RCaMP1h (pseudocolored) and Lifeact-GFP (overlaid in insets; gray), before and after exposure to 40 mM KCl at t = 0 s. Pancreatic islets were infected with Ad-Lifeact-GFP and AAV1-RCaMP1h for 2 hr, washed, and cultured for 96 hr. The islets were then washed and resuspended in KRB medium with low KCl (4.7 mM) and 3 mM glucose for 45 min before imaging. Insets are reduced in size by 3.5×. Yellow arrows point to the vertex of the stimulated cell, displaying enhanced elevation in Ca^{2+} levels over time. The nucleus is marked with asterisks. Oblique lines in (A) and (A'), plotted through a nonedge cortical segment (turquoise) and through an edge (magenta), were used to generate the kymographs in (B). The kymographs are oriented so that the bottom of the panels corresponds to the cell interior.

(C–D') β cells expressing Lifeact-GFP (gray, upper panels) and RCaMP1h (pseudocolored), before and after KCl stimulation. Arrows point to three edges displaying enhanced elevation in their Ca^{2+} levels. Asterisks mark nuclei.

(E) Elevation in Ca^{2+} levels ($\Delta f/f_0$) following KCl stimulation at the edges and adjacent flat areas of the β cell surface (nonedge). Each circle represents $\Delta f/f_0$ values from an individual β cell. These values were obtained by averaging at least three edge and nonedge 1–1.5µm cortical segments ($p = 3 \times 10^{-11}$; paired sample; t test [two tailed]; n = 40 cells from 17 islets imaged in four independent experiments [sets of mice]). Note that nearly all circles fall above the oblique line, demonstrating that elevation in Ca^{2+} levels is consistently greater near cell edges.

(F) $\Delta f/f_0$ ratios between edges and nonedge segments following KCl stimulation of the values depicted in (C). Each circle represents the ratio between the averaging of at least three edges compared with three nonedged segments in an individual β cell (n = 40 cells from 17 islets imaged in four independent experiments [sets of mice]). Center lines show the medians; box limits indicate the 25th and 75th percentiles as determined by R software; whiskers extend 1.5 times the interquartile range from the 25th and 75th percentiles. The scale bars represent 5 µm.

are essential for coordinating the secretory activity at each rosette and between rosettes (Bavamian et al., 2007). This gap junction communication may be optimized by preferential contact at the edges, which are enriched for sensing and secretory elements.

EXPERIMENTAL PROCEDURES

Isolation and Culture of Mouse Pancreatic Islets, Preparation of Mouse Whole-Pancreas Fragments, and Culturing of Human Islets

Mice were handled according to Institutional Animal Care and Use Committee guidelines. Isolated mouse pancreatic islets were prepared as described previously (Carter et al., 2009). In brief, 8- to 12-week-old mice were euthanized and their pancreata were perfused with oxygenated Hanks' balanced salt solution (HBSS) supplemented with Collagenase P (Roche; 0.75 mg/ml). Excised tissue was digested, washed thoroughly, and filtered. Pancreatic islets were separated from the exocrine tissue by a Histopaque gradient. For whole-pancreas preparations of C57BL/6 and Lifeact-GFP mice, pancreata were excised without collagenase digestion, rinsed in HBSS/BSA, and minced by scissors to ~1 mm fragments. These fragments were then immediately fixed in 4% paraformaldehyde in PBS for 45 min.

Isolated human islets (>90% purity) were provided by the European Consortium for Islets Transplantation Islet for Basic Research program through a Juvenile Diabetes Research Foundation award 31-2008-413. Islets were of brain-dead nondiabetic adult donors (age 43 ± 2 years; body mass index 26.9 ± 0.9 kg/m^2; n = 2). Human islets studies received Ethics Committee approval.

Microscopy

Data were acquired with LSM510, LSM710, and LSM780 confocal imaging systems (Zeiss) equipped with 60×/1.4 or 100×/1.4 objectives. For live imaging experiments, islets were loaded onto ibidi microslides (ibidi; 80826) uncoated or coated with Matrigel (BD Biosciences).

SUPPLEMENTAL INFORMATION

Supplemental Information includes Supplemental Experimental Procedures, five figures, and five movies and can be found with this article online at http://dx.doi.org/10.1016/j.celrep.2014.12.031.

ACKNOWLEDGMENTS

We thank the members of the Shilo laboratory for fruitful input and Yuval Dor, Danny Ben-Zvi, and Michael Walker for valuable discussions and critical reading of the manuscript. We thank Yehiel Zick for a fruitful collaboration. We also thank Loren Looger for AAV-RCaMPh1 and Amitai Mandelbaum for technical help. This work was supported by US-Israel Binational Science Foundation grants to E.D.S. and B.-Z.S. and by grants from the Administral Anslat Foundation, Kekst, and Shapell to B.-Z.S., who is an incumbent of the Hilda and Cecil Lewis Chair in Molecular Genetics.

Received: September 3, 2014
Revised: November 11, 2014
Accepted: December 12, 2014
Published: January 15, 2015

REFERENCES

Akerboom, J., Carreras Calderón, N., Tian, L., Wabnig, S., Prigge, M., Tolö, J., Gordus, A., Orger, M.B., Severi, K.E., Macklin, J.J., et al. (2013). Genetically

encoded calcium indicators for multi-color neural activity imaging and combination with optogenetics. Front. Mol. Neurosci. *6*, 2.

Ashcroft, F.M., and Rorsman, P. (2012). Diabetes mellitus and the β cell: the last ten years. Cell *148*, 1160–1171.

Bavamian, S., Klee, P., Britan, A., Populaire, C., Caille, D., Cancela, J., Charollais, A., and Meda, P. (2007). Islet-cell-to-cell communication as basis for normal insulin secretion. Diabetes Obes. Metab. *9* (*Suppl 2*), 118–132.

Bendayan, M. (1992). Association of secreted insulin with particular domains of the pancreatic B-cell plasma membrane: the actin-rich microvilli. J. Histochem. Cytochem. *40*, 327–331.

Bonner-Weir, S. (1988). Morphological evidence for pancreatic polarity of beta-cell within islets of Langerhans. Diabetes *37*, 616–621.

Carter, J.D., Dula, S.B., Corbin, K.L., Wu, R., and Nunemaker, C.S. (2009). A practical guide to rodent islet isolation and assessment. Biol. Proced. Online *11*, 3–31.

Carvell, M.J., Marsh, P.J., Persaud, S.J., and Jones, P.M. (2007). E-cadherin interactions regulate beta-cell proliferation in islet-like structures. Cell. Physiol. Biochem. *20*, 617–626.

Dahl, U., Sjødin, A., and Semb, H. (1996). Cadherins regulate aggregation of pancreatic beta-cells in vivo. Development *122*, 2895–2902.

Drews, G., Krippeit-Drews, P., and Düfer, M. (2010). Electrophysiology of islet cells. Adv. Exp. Med. Biol. *654*, 115–163.

Gembal, M., Gilon, P., and Henquin, J.C. (1992). Evidence that glucose can control insulin release independently from its action on ATP-sensitive K+ channels in mouse B cells. J. Clin. Invest. *89*, 1288–1295.

Geron, E., Schejter, E.D., and Shilo, B.Z. (2013). Directing exocrine secretory vesicles to the apical membrane by actin cables generated by the formin mDia1. Proc. Natl. Acad. Sci. USA *110*, 10652–10657.

Granot, Z., Swisa, A., Magenheim, J., Stolovich-Rain, M., Fujimoto, W., Manduchi, E., Miki, T., Lennerz, J.K., Stoeckert, C.J., Jr., Meyuhas, O., et al. (2009). LKB1 regulates pancreatic beta cell size, polarity, and function. Cell Metab. *10*, 296–308.

Halban, P.A., Wollheim, C.B., Blondel, B., Meda, P., Niesor, E.N., and Mintz, D.H. (1982). The possible importance of contact between pancreatic islet cells for the control of insulin release. Endocrinology *111*, 86–94.

Hauge-Evans, A.C., Squires, P.E., Persaud, S.J., and Jones, P.M. (1999). Pancreatic beta-cell-to-beta-cell interactions are required for integrated responses to nutrient stimuli: enhanced Ca2+ and insulin secretory responses of MIN6 pseudoislets. Diabetes *48*, 1402–1408.

Henquin, J.C. (2009). Regulation of insulin secretion: a matter of phase control and amplitude modulation. Diabetologia *52*, 739–751.

Kasai, H., Hatakeyama, H., Ohno, M., and Takahashi, N. (2010). Exocytosis in islet beta-cells. Adv. Exp. Med. Biol. *654*, 305–338.

Konstantinova, I., and Lammert, E. (2004). Microvascular development: learning from pancreatic islets. Bioessays *26*, 1069–1075.

Konstantinova, I., Nikolova, G., Ohara-Imaizumi, M., Meda, P., Kucera, T., Zarbalis, K., Wurst, W., Nagamatsu, S., and Lammert, E. (2007). EphA-Ephrin-A-mediated beta cell communication regulates insulin secretion from pancreatic islets. Cell *129*, 359–370.

Low, J.T., Zavortink, M., Mitchell, J.M., Gan, W.J., Do, O.H., Schwiening, C.J., Gaisano, H.Y., and Thorn, P. (2014). Insulin secretion from beta cells in intact mouse islets is targeted towards the vasculature. Diabetologia *57*, 1655–1663.

Ma, H., Groth, R.D., Cohen, S.M., Emery, J.F., Li, B., Hoedt, E., Zhang, G., Neubert, T.A., and Tsien, R.W. (2014). γCaMKII shuttles Ca^{2+}/CaM to the nucleus to trigger CREB phosphorylation and gene expression. Cell *159*, 281–294.

Meda, P., Bosco, D., Chanson, M., Giordano, E., Vallar, L., Wollheim, C., and Orci, L. (1990). Rapid and reversible secretion changes during uncoupling of rat insulin-producing cells. J. Clin. Invest. *86*, 759–768.

Ohara-Imaizumi, M., Aoyagi, K., Nakamichi, Y., Nishiwaki, C., Sakurai, T., and Nagamatsu, S. (2009). Pattern of rise in subplasma membrane Ca2+ concentration determines type of fusing insulin granules in pancreatic beta cells. Biochem. Biophys. Res. Commun. *385*, 291–295.

Orci, L., Thorens, B., Ravazzola, M., and Lodish, H.F. (1989). Localization of the pancreatic beta cell glucose transporter to specific plasma membrane domains. Science *245*, 295–297.

Riedl, J., Crevenna, A.H., Kessenbrock, K., Yu, J.H., Neukirchen, D., Bista, M., Bradke, F., Jenne, D., Holak, T.A., Werb, Z., et al. (2008). Lifeact: a versatile marker to visualize F-actin. Nat. Methods *5*, 605–607.

Rutter, G.A., Tsuboi, T., and Ravier, M.A. (2006). Ca2+ microdomains and the control of insulin secretion. Cell Calcium *40*, 539–551.

Sadoul, K., Lang, J., Montecucco, C., Weller, U., Regazzi, R., Catsicas, S., Wollheim, C.B., and Halban, P.A. (1995). SNAP-25 is expressed in islets of Langerhans and is involved in insulin release. J. Cell Biol. *128*, 1019–1028.

Takahashi, N., Kishimoto, T., Nemoto, T., Kadowaki, T., and Kasai, H. (2002). Fusion pore dynamics and insulin granule exocytosis in the pancreatic islet. Science *297*, 1349–1352.

Thorens, B., Sarkar, H.K., Kaback, H.R., and Lodish, H.F. (1988). Cloning and functional expression in bacteria of a novel glucose transporter present in liver, intestine, kidney, and beta-pancreatic islet cells. Cell *55*, 281–290.

Weir, G.C., and Bonner-Weir, S. (1990). Islets of Langerhans: the puzzle of intraislet interactions and their relevance to diabetes. J. Clin. Invest. *85*, 983–987.

Xia, F., Gao, X., Kwan, E., Lam, P.P., Chan, L., Sy, K., Sheu, L., Wheeler, M.B., Gaisano, H.Y., and Tsushima, R.G. (2004). Disruption of pancreatic beta-cell lipid rafts modifies Kv2.1 channel gating and insulin exocytosis. J. Biol. Chem. *279*, 24685–24691.